



Effect of Preheating on Combustion Characteristics of a Swirling Flameless Combustor

Najib Aminu Ismail, Raid Abid Alwan, Mazlan Abdul Wahid,
Aminuddin Saat and Mohammed Bashir Abdulrahman

EasyChair preprints are intended for rapid dissemination of research results and are integrated with the rest of EasyChair.

October 27, 2021

Effect of Preheating on Combustion Characteristics of a Swirling Flameless Combustor

Najib Aminu Ismail^{1,2, a)} Raid Abid Alwan^{1, b)} Mazlan Abdul Wahid^{1, c)} Aminuddin Sa'at^{1, d)} Mohammed Bashir Abdulrahman^{1, e)}

¹High Speed Reacting Flow Laboratory, School of Mechanical Engineering, Universiti Teknologi Malaysia

²Department of Mechanical Engineering, Ahmadu Bello University, Zaria

a) Corresponding author: njbslm01@gmail.com

b) raidcombustion@gmail.com

c) mazlan@mail.fkm.utm.my

d) aminudin@utm.my

e) mobash2007@gmail.com

Abstract. Flameless combustion is a state-of-the-art combustion technique that provides uniform temperature distribution while increasing efficiency and reducing emissions. An internally preheated swirling flameless burner (IPSFC) operating in flameless mode has been developed and tested to provide improved combustion characteristics and very low pollutant emissions. The IPSFC burner was operated at a heat input of 7 kW to 15 kW with a preheated combustion temperature. In the study, the effects of combustion air with and without preheating on gaseous fuel combustion characteristics are investigated for the six cases: SFR2, SFR4, SFR42, PSFR2, PSFR4 and PSFR42. The results show that the best configuration for a flameless burner is the SFR42 case, a vortex burner with four tangential air inlets, 12 axial air inlets, and 11 coaxial fuel inlets. The preheated air was found to increase the thermal efficiency of the process by about 10% compared to the process without preheating but at the cost of a small increase in NO_x emissions. At an equivalence ratio of 0.8, the lowest NO_x and CO emissions were found to be 3 ppm and 24 ppm, respectively. Temperature uniformity varied from 0.03 in SFR42 to 0.04 in SFR2 at different equivalence ratios.

INTRODUCTION

Combustion processes are used to produce heat and power, which are essential components of our daily life. The combustion process is characterized by a series of exothermic processes. The energy held in fuel's chemical bonds are converted to heat energy, which can be used in a variety of applications such as heavy industries and power plant, to generate the necessary steam for turbines, which then produce heat and electricity [1]. The population of the world is growing significantly and hence energy demand is increasing due to economic developments in countries like China and India [2] and [3]. This process results in excessive heat generation and increased global warming. The issue of global warming is really important and needs to be addressed. A permanent shift in the earth's climate is projected due to the gradual increase in the average temperature of the planet. Human civilization is under grave danger as a result of this transformation [4]. The emissions of potential pollutants and greenhouse gases are linked to the combustion of fossil fuels, which is the primary cause of global warming [3,5]. Various researches have been done to reduce the formation of such harmful gases [6]. As a result, lowering combustion emissions and increasing combustion system thermal efficiency are significant problems in the design of thermal energy and power systems.

Several combustion strategies have been developed to reduce polluting gas emissions [7]. One of these methods is flameless combustion, it is important to know that flameless combustion has various characteristics that differs from conventional combustion [8–11]. The absence of a high-temperature flame front is the most unique aspect of flameless combustion. Flameless combustion has a number of advantages over conventional combustion models, including minimal combustor pressure oscillation, which minimizes noise, excellent combustion efficiency, which helps to reduce energy consumption, and, most critically, exceptionally low polluting exhaust emissions [12]. The reaction occurs consistently across the combustion chamber, considerably below the temperature at which N₂ dissociates, decreasing NO_x generation. This type of combustion has low oxygen content, which is lower than that found in the atmosphere. Slower chemical reaction rates, homogeneous temperature distribution, larger reaction zones, and an unseen flame characterize the ignition process. The concept of exhaust gas and heat recirculation serves as the technique's basic operating premise. The heat from the exhaust gases is utilized to raise the temperature of the oxidant stream [13,14] while the exhaust gases are used to dilute the oxidant stream and so lower the oxygen concentration in the combustion zone to maintain a low temperature. Less NO is produced as a result of this method [15]. When compared to conventional flames, the term "flameless" refers to the lack of visible signature from the flames.

Flameless combustion is a promising technique that combines high efficiency with extremely low emissions. It is based on high flue gas recirculation and fuel and oxidizer mixing. Internal recirculation entrains the flue gas from the separated fuel, which has a high velocity. As a result, the amount of oxygen in the combustion zone is reduced and chemical energy is released at a more evenly distributed rate, avoiding high peak temperatures and lowering polluting emissions. A high recirculation ratio requires the high-speed jet of the oxidizer (with or without preheating) or of the fuel [16]. Internal and exterior flue gas recirculations (FGR) are the two types of FGR. The former is based on burner design, whereas the latter is based on an external pipe returning flue gas to the combustor. The flue gases are cycled back to the combustor in the internal FGR due to the burner aerodynamics. In combustion operations, recirculation and good mixing of air and fuel are critical. During swirl flow, a similar process is employed to induce recirculation and stabilize the combustion. This is important because it allows the hot combustion products to be recirculated back to the flame source. The creation of whirling combustion by tangential air entry in a cylindrical combustor is one of the ways employed for that procedure. Without the use of a flame stabilizer, swirling flameless combustion is used in a direct injection of both air and fuel. Air is injected tangentially and axially to impart swirling without the need of swirlers, which are generally employed in conventional combustors, to create an auto swirling process. The ultra-low pollutant emissions, homogenous temperature inside the combustion chamber and stable combustion are all advantages of flameless combustion technology. Environmental difficulties in power generation play a significant role in the economic viability of power plants, especially in light of today's stringent emission restrictions. The current trend is to create industrial combustion devices with high efficiency and low emissions in order to eliminate harmful emissions. NO_x produced by combustion operations is one of these hazardous emissions. The design and implementation of flameless combustion is one of the most effective strategies for lowering NO_x. There are two key needs to meet in order to accomplish flameless combustion [17]. That is, the combustion temperature inside the chamber should be higher than the mixture's auto ignition temperature (800 °C for natural gas/air [17,18]). and the flue-gas recirculation ratio (Kv) between the fuel, the oxidizer, and the diluted gas (flue gas, N₂, or CO₂) should be more than three (>3) [17][19].

The ability to provide proper mixing between the entering fresh fuel/air mixture and the re-circulated hot burnt gases is critical for the efficient construction of a flameless combustor. For flameless combustion, adequate and rapid mixing between the injected air and the internally recirculated hot reactive gases to generate a hot and diluted oxidant, followed by rapid mixing with fuel, is crucial. To obtain the high circulation required for flameless combustion, many researchers employed diluted gases like CO₂ and/or N₂ fed into the combustion chamber. Swirl is a natural phenomenon that aids combustion. To create swirl, many studies employed vanes or tangential entrance [10,20,21]. Using an asymmetric vortex combustor, several researchers advocated introducing swirl with tangential entrance. The asymmetric vortex combustor, on the other hand, has an issue with the low temperature zone in the centre [22]. This is not ideal for combustion without the use of a flame. The axial thrust of the reacting flow within the combustor is critical, and it is usually accomplished by producing a swirl motion caused by the interplay of axial and tangential air velocity components. A new design for a flameless combustor with high recirculation for quick mixing is offered in this study. As a result, while being a non-premixed flame, the vortex flame exhibits the aesthetic qualities of a premixed flame.

This research has practical applications in the manufacturing industry in general, and in gas turbines in particular. It also makes a substantial contribution to addressing the issue of global warming and reducing ozone depletion. It also assists relevant sectors, such as gas turbines, in achieving more efficient combustion processes. Without the use of gas dilution, new combustor architecture is designed to accomplish swirling flameless

combustion (e.g N₂, CO₂ etc.). This study focuses on the newly designed asymmetric swirling flow combustion system. The objectives of this present work are: To investigate experimentally the effects of multiple air-fuel injection configurations on swirling flameless and to investigate the effect of air preheating on thermal efficiency of swirling flameless combustion.

MATERIALS AND METHOD

For testing purposes, the burner was built to run in vortex and swirling combustion modes as well as flameless mode. Natural gas was used to power the burner at a thermal load of 12kW in stoichiometry for both flame and flameless modes. The air was directed to travel within the helical stainless steel pipe fixed inside the combustion chamber to pre-heat tangential air from the air supply system. As a result, the temperature of the air delivered was raised to 600 degrees Fahrenheit. For certain fuels, this preheating device is necessary to keep the inside of the combustor above the auto ignition temperature.

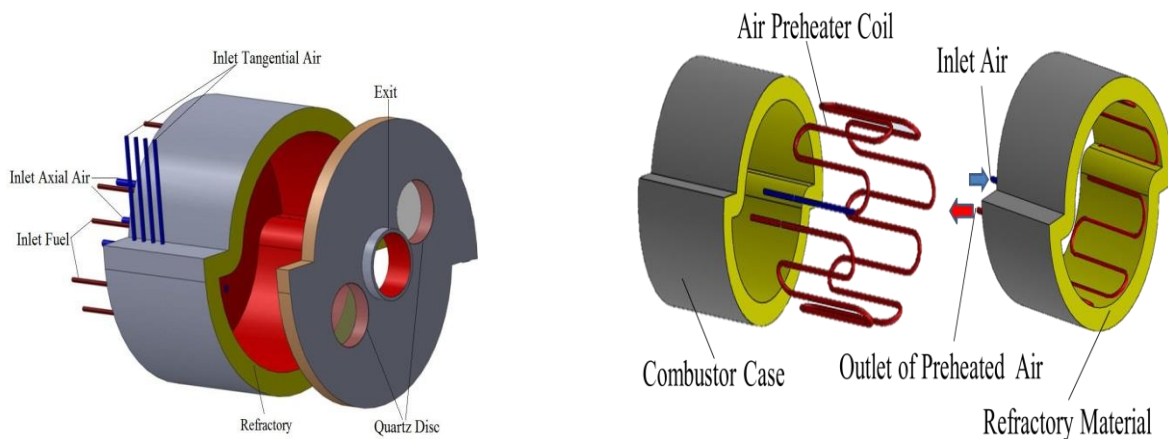


FIGURE 1. (a) Schematic of the swirling flameless combustor, (b) Internally air preheat system

As illustrated in Figure 3.2, the test rig is equipped with multiple instrumentation units for recording the following variables. Flow meters were used to measure the air and fuel flow rates. The equivalence ratio can be changed by altering the inlet mass flow rate of air and fuel. In the current experiment, the fuel was natural gas, with methane accounting for around 92 percent of the fuel content. S-type thermocouples were used to measure the temperature of the preheated air and the temperature of the midplane along the combustion chamber (TC). Temperature measurements are taken through six holes. The first hole is 60 mm away from the burner, while the second, third, fourth, fifth, and sixth holes are 90, 120, 150, 210, and 270 mm away from the burner, respectively. Air is supplied at 2 bar pressure by a compressor with a dampening tank. The natural gas used has a heating value of 35.0 MJ/Kg and is supplied under 4.5 bar pressure from a pressurized tank while the air for this experiment was supplied by two air compressors, one of which provided tangential air and the other axial air.

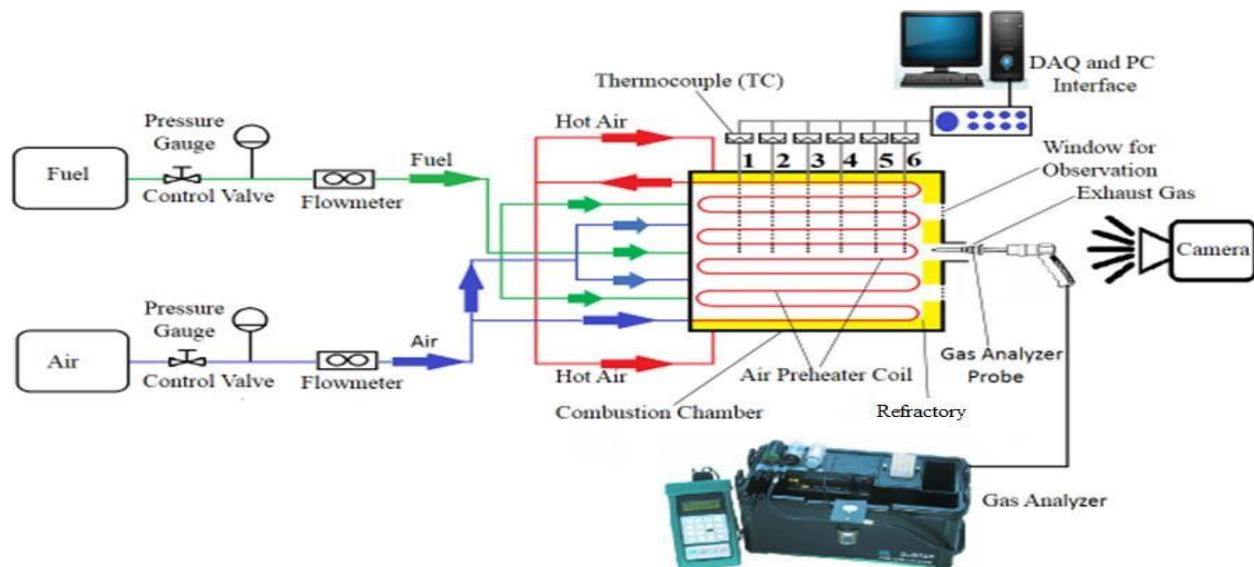


FIGURE 2. Experimental set up for swirling flameless combustion

EXPERIMENTAL MEASUREMENT

During the experiment, the flow measurement system used variable area flow meters to monitor flow rates in the flow metres for air and fuel. The flow of natural gas was measured using two Cole Parmer flow metres (maximum 3286.8 mL/min, minimum 231.3 mL/min, and standard accuracy). To measure air flow, six Dwyer VFB- 55 flow meters with a maximum flow rate of 200 standard cubic feet per hour (SCFH) and standard accuracy were utilized. Manufacturers of various area flow meters state that full-scale readings must be accurate to within 2% of maximum flow and have a repeatability rate of 0.25 percent. Near-full-scale operation is recommended for this class of metres. Five quick-disconnect S-type thermocouples (maximum range -50°C to $+1760^{\circ}\text{C}$, accuracy: 1.5°C or 0.25 percent of reading, whichever is larger) were inserted within the combustion chamber to monitor the furnace's temperature profile. A K-type thermocouple was inserted at the air nozzle input to measure air temperature during flameless combustion (maximum range: -100°C to $+1370^{\circ}\text{C}$, accuracy: 2°C or 0.75 percent of reading, whichever is greater). In the middle of the combustion chamber, an S-type thermocouple was installed. A Picolog data collecting system was used to record all temperatures (TC-08). Temperature measurements were taken with a TC-08 thermocouple data logger, which performed quickly and accurately. The TC-08 is linked to thermocouples and wired into a USB port on the computer to collect temperature data. The temperature range of the TC-08 is -270°C to $+1820^{\circ}\text{C}$. The TC-08's quick conversion time (less than a second) allows for up to ten temperature measurements per second. The TC-08, on the other hand, can detect minute temperature changes because to its high resolution (20 bits).

In this investigation, it is critical to measure gas emissions. Microprocessor-based gas analyzers make up a large part of the product line. To assess flue within the exhaust hole for the current project, we used a KM9106 Quintox gas analyzer. The KM9106 Quintox includes long and short probes that can evaluate flue gas components within 5 minutes of direct contact with the exhaust and can sample NOX, CO, and oxygen content every 5 minutes. A 1-meter-long temperature probe (sensitive to 1200°C) is also included with the gas analyzer, allowing for safe monitoring of flameless combustor gas emissions. A KM9106 Quintox gas analyzer is used to measure exhaust gas emissions. A KM9106 Quintox gas analyzer was used to measure pollutant emissions inside the exhaust hole for this study.

Cases Investigated

All the cases investigated in this research are summarized in the table 1 below. The case name indicates the axial air and fuel injection location, as well as the combustion mode. Case SA8F4 denotes vortex combustion with eight inlet air ports and four fuel injection ports; SFR4 denotes a swirling flameless combustion at the site of the axial air inlet, organized symmetrically around the centre of the burner with distance (R/4). In each side of the cylinder, two ports of inflow tangential air and five ports of fuel were used to explore swirling flameless combustion, as shown in Figure 3. The following are the variables that were used in the experiments:

TABLE 1. Experimental parameters used to investigate swirling flameless combustor

Cases		Location of axial air	Total air				Equivalence ratio
			Axial air		Tangential air		
			Flow rate	Numbers of ports	Flow rate	Numbers of ports	
Without preheat air	SFR4	R/4	50 %	6	50 %	4	0.5-1.2
	SFR2	R/2	50 %	6	50 %	4	0.5-1.2
	SFR42	R/4 and R/2	50 %	12	50 %	4	0.5-1.2
With preheat air (T=600 K)	PSFR4	R/4	50 %	6	50 %	4	0.5-1.2
	PSFR2	R/2	50 %	6	50 %	4	0.5-1.2
	PSFR42	R/4 and R/2	50 %	12	50 %	4	0.5-1.2

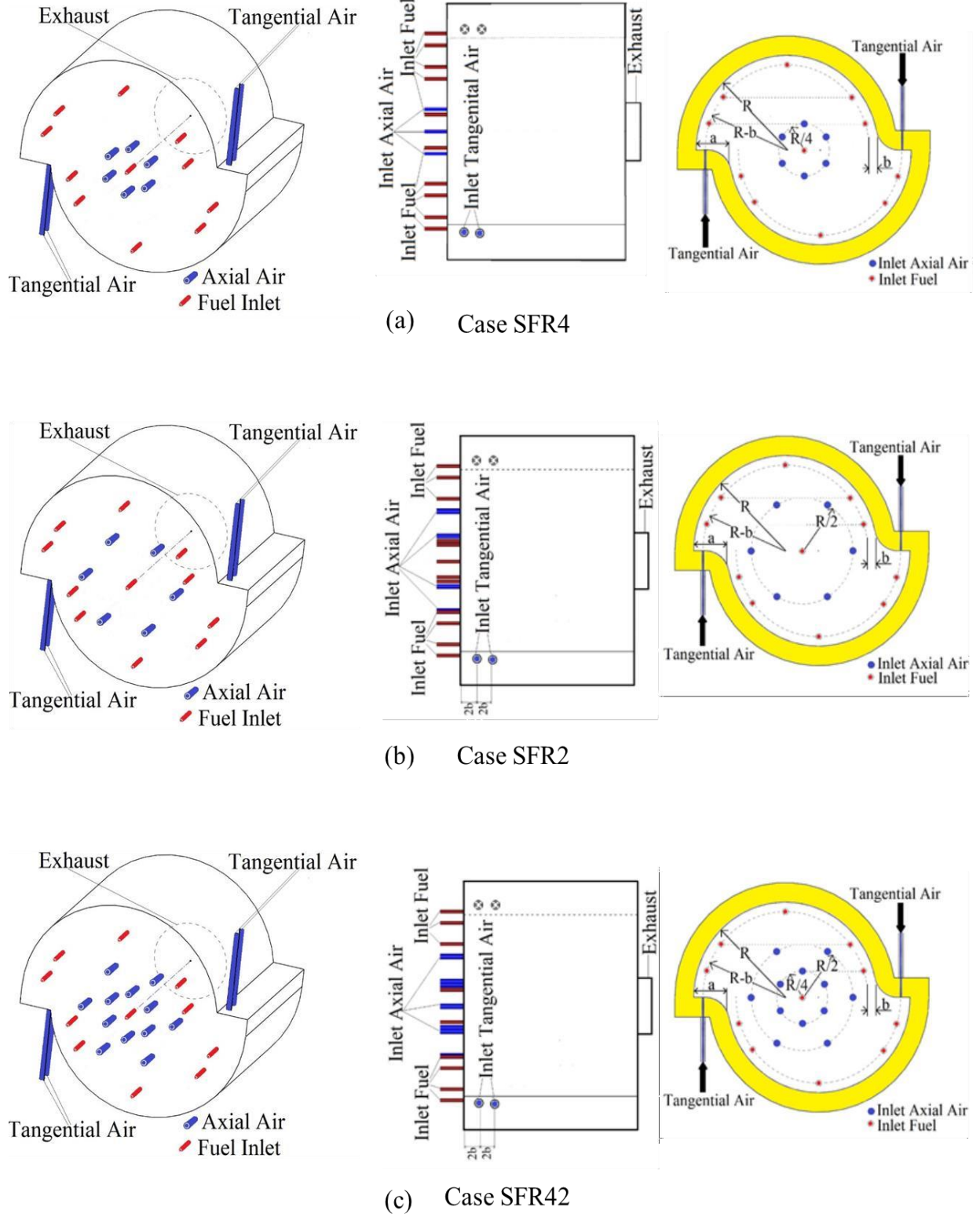


FIGURE 3. Locations of air and fuel in swirling combustor for (a) Case SFR2, (b) Case SFR4 and (c) Case SFR42

Thermal Efficiency

The thermal efficiency of a process determines how well it converts or transfers energy. In general, thermal efficiency is defined as the energy ratio between a device's useful output and its input. The following is a generic definition of thermal efficiency:

$$\text{Thermal Efficiency, } \eta_{\text{th}} = \frac{Q_{\text{out}}}{Q_{\text{in}}} \quad (1)$$

$$\eta_{\text{th}} = \frac{Q_{\text{out}}}{Q_{\text{in}}} = \frac{\dot{m}_a \cdot C_{p_a} \cdot (T_{\text{out}} - T_{\text{in}}) \cdot \left(1 + \frac{\dot{m}_f}{\dot{m}_a}\right)}{\dot{m}_f \cdot LHV} \quad (2)$$

where \dot{m}_a , C_{p_a} , \dot{m}_f , and LHV are the air mass flow rate, specific heat for air, fuel mass flow rate and the lower heat value for fuel, respectively.

Experimental Procedure

LPG was used to preheat the combustion chamber for around 1 hour in all experiments with swirling flameless combustion. The typical flame continued to burn natural gas once the combustion chamber was heated up. The furnace was heated with a normal flame until the threshold temperature was attained in order to establish flameless combustion. The fuel was then turned back on when the flame had quenched, which took less than a minute. The furnace temperature was kept above the threshold temperature during this operation. This is due to the fact that the flameless combustion regime is highly dependent on ambient temperature, which must be high enough to maintain chemical reactions in the absence of a flame front. The average furnace midplane temperature was above 1200 K in this investigation, resulting in stable natural gas combustion. This temperature was higher than the natural gas auto ignition temperature.

RESULTS AND DISCUSSION

As shown in Table 1, six scenarios are considered depending on tangential air preheat: three with preheat PSFR4, PSFR2, and PSFR42, and three without preheat SFR4, SFR2, and SFR42. The increased temperature of the air inlet is expected to have a significant impact on combustion kinetics, pollutant production, and emissions. A greater flame temperature is caused by a higher air intake temperature. Experiments were carried out with equivalency ratios ranging from 0.5 to 1.2. The findings were used to compare the performance of the combustor with and without a 600 K warmed tangential air temperature.

Temperature Distribution

At stoichiometric equivalence ratios, Figure 4 illustrates the temperature profiles along the central axis for instances with preheated tangential air PSFR4, PSFR2, and PSFR42, and cases without preheated tangential air SFR4, SFR2, and SFR42. It demonstrates that flameless combustion is possible with or without preheated air if the temperature within the chamber is higher than the fuel's auto ignition temperature. All cases of preheated tangential air (PSFR4, PSFR2, and PSFR42) had greater temperatures than cases without preheated tangential air (SFR4, SFR2, and SFR42). The temperature of the air input had a significant impact on combustion kinetics, pollutant production, and emissions. Higher flame temperatures are caused by higher air inlet temperatures. However, because recirculation increased air-fuel mixing by reducing the local high temperature zone, the temperature distribution is determined to be evenly reduced toward the combustor outlet in all circumstances. At stoichiometric equivalence ratio, the

maximum temperature for Case PSFR42 was found to be higher than for the other Cases. This is because the whirling in Case SFR42 resulted in good air-fuel mixing and recirculation to finish the combustion.

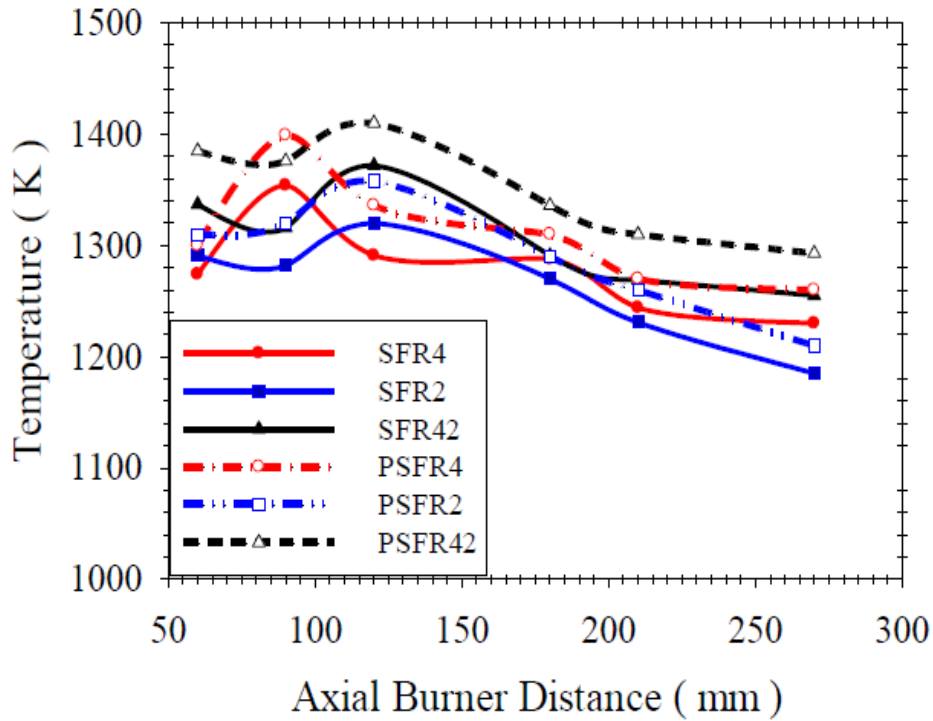


FIGURE 4. Temperature distribution along the central axis for case with and without preheat tangential air at stoichiometric equivalence ratio.

The average NO_x emission for the swirling flameless examples SFR4 and PSFR4 is shown in Figure 5. The NO_x emission during flameless combustion was always less than 14 ppm, as shown in this graph. The NO_x emission was lower in the absence of preheated air, due to low temperatures in the combustion chamber. The NO_x concentration in the lean cases is lower than in the rich and stoichiometric cases, based on these findings. Cases SFR2 and PSFR2, as shown in Figure 6, and cases SFR42 and PSFR42, as shown in Figure 7, experienced the same circumstance. With and without preheated tangential air, case SFR42 had the lowest NO_x emission.

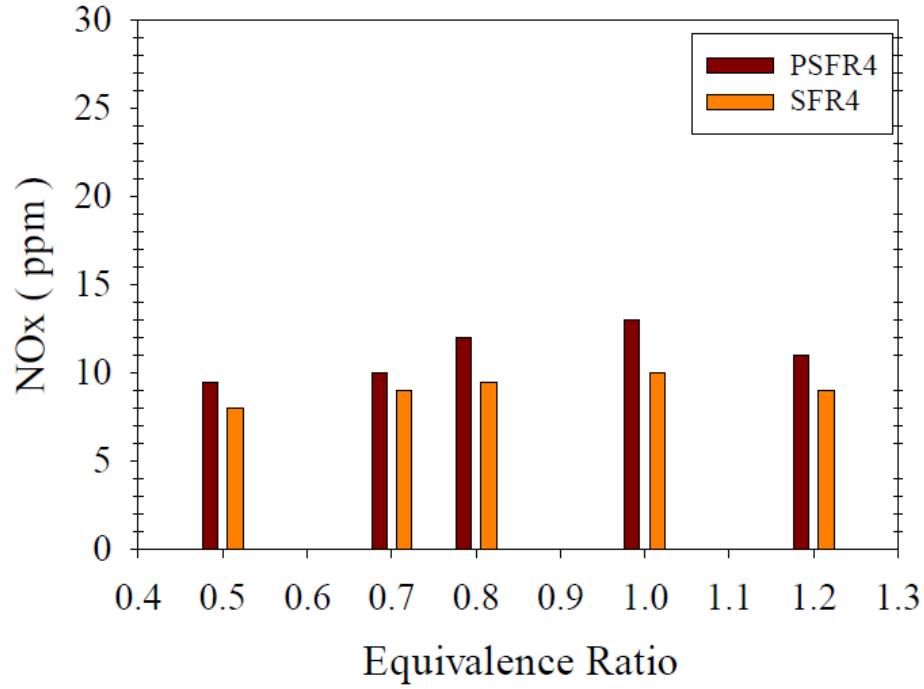


FIGURE 5. Average NO_x concentrations plotted against equivalence ratio for cases with and without preheated tangential air, PSFR4 and SFR4, respectively.

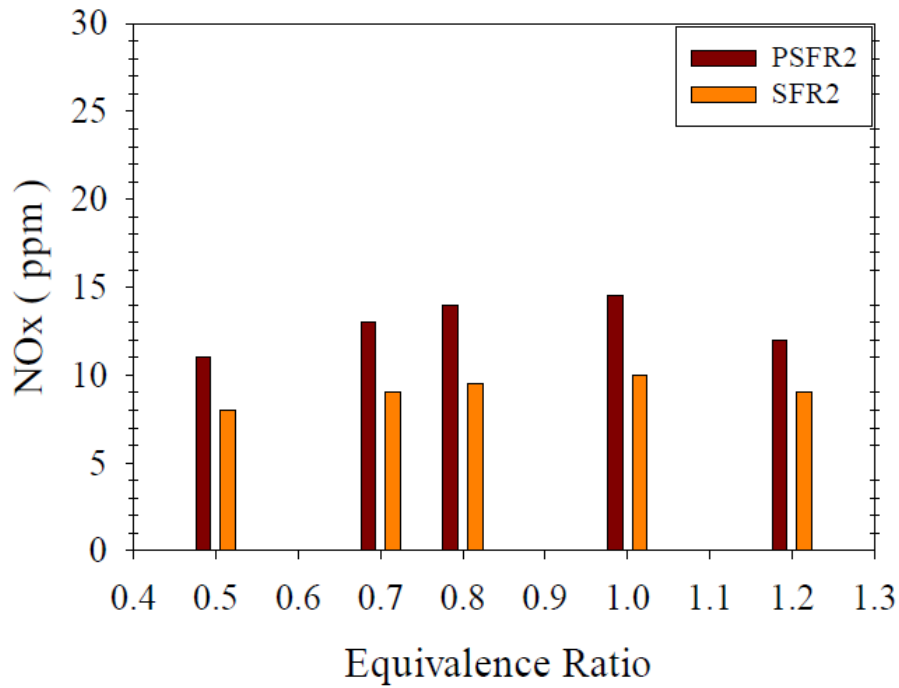


FIGURE 6. Average NO_x concentrations plotted against equivalence ratio for cases with and without preheated tangential air, PSFR2 and SFR2, respectively.

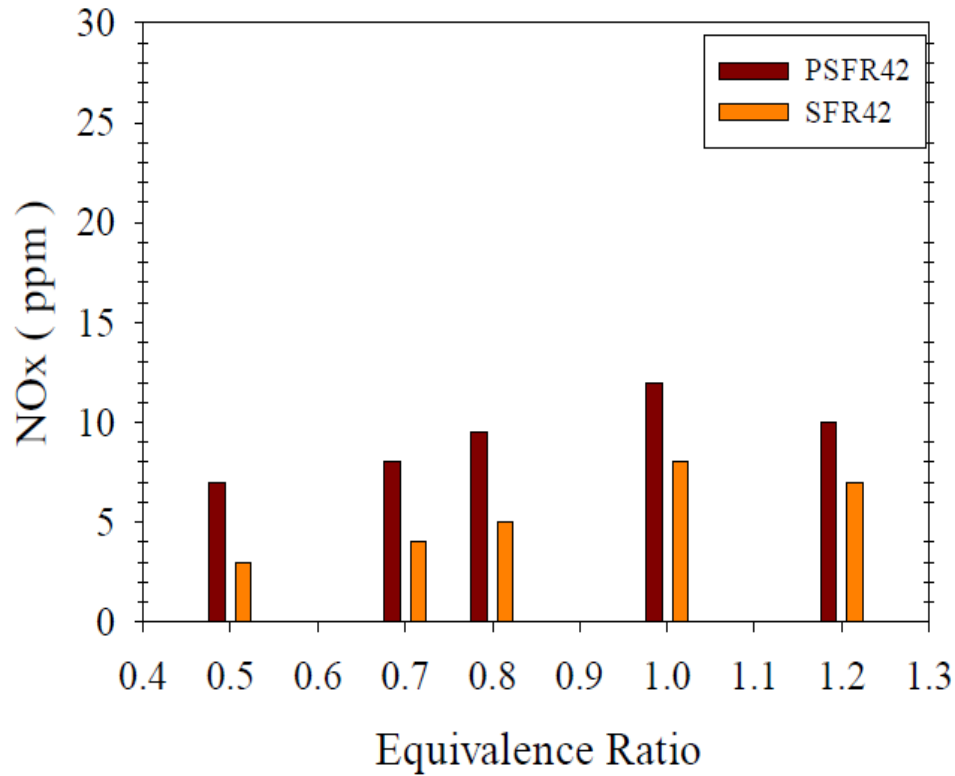


FIGURE 7. Average NOX concentrations plotted against equivalence ratio for cases with and without preheated tangential air, PSFR42 and SFR42, respectively.

The average CO emission concentrations for cases SFR4 (without preheated tangential air) and PSFR4 (with preheated tangential air) for various equivalence ratios are shown in Figure 8. At stoichiometric equivalence ratio, CO emission was less than 60 ppm for case SFR4 and 55 ppm for case PSFR4 during flameless combustion. At various equivalence ratios, the CO emission in the case with preheated air was lower than the case without preheated air. It's worth noting that a greater air inlet temperature leads to a higher flame temperature, which speeds up the conversion of CO to CO₂. CO emissions have fallen considerably, which is a good thing. The drop in CO is due to the fact that as the flame temperature rises, the conversion of CO to CO₂ accelerates, resulting in less CO in the product gases. As illustrated in Figures 9 and 10, this was repeated for cases PSFR2 and PSFR42, respectively. In all of these graphs, the lowest CO value was recorded in lean combustion (equivalence ratio = 0.8).

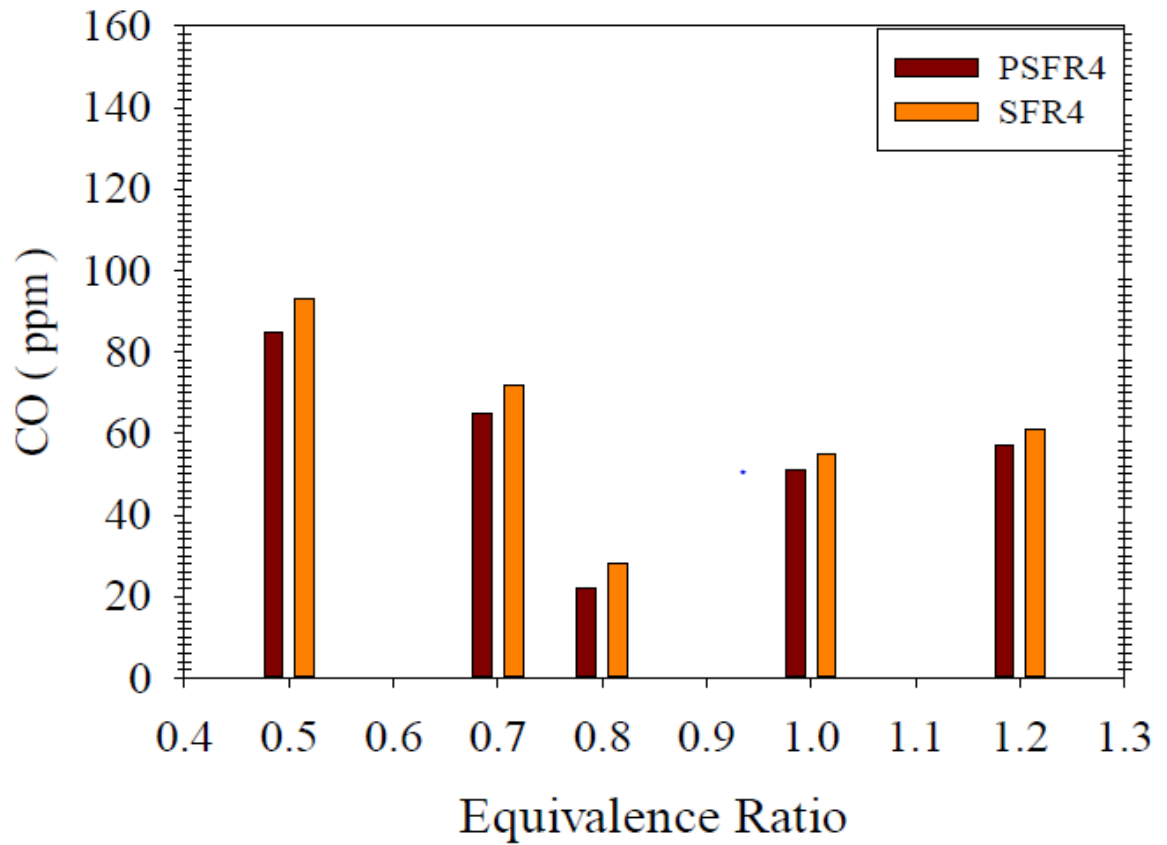


FIGURE 8. Average CO concentrations plotted against equivalence ratio for cases with and without preheated tangential air, PSFR4 and SFR4, respectively

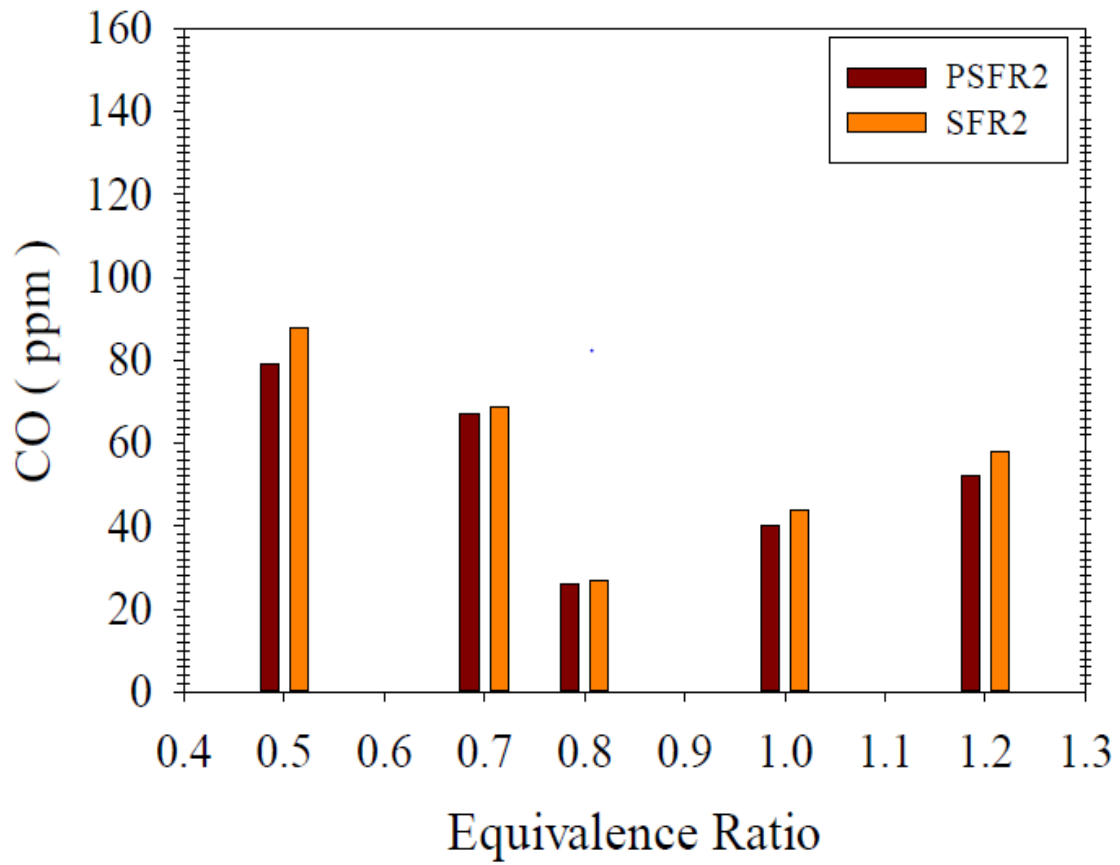


FIGURE 9. Average CO concentrations plotted against equivalence ratio for cases with and without preheated tangential air, PSFR2 and SFR2, respectively.

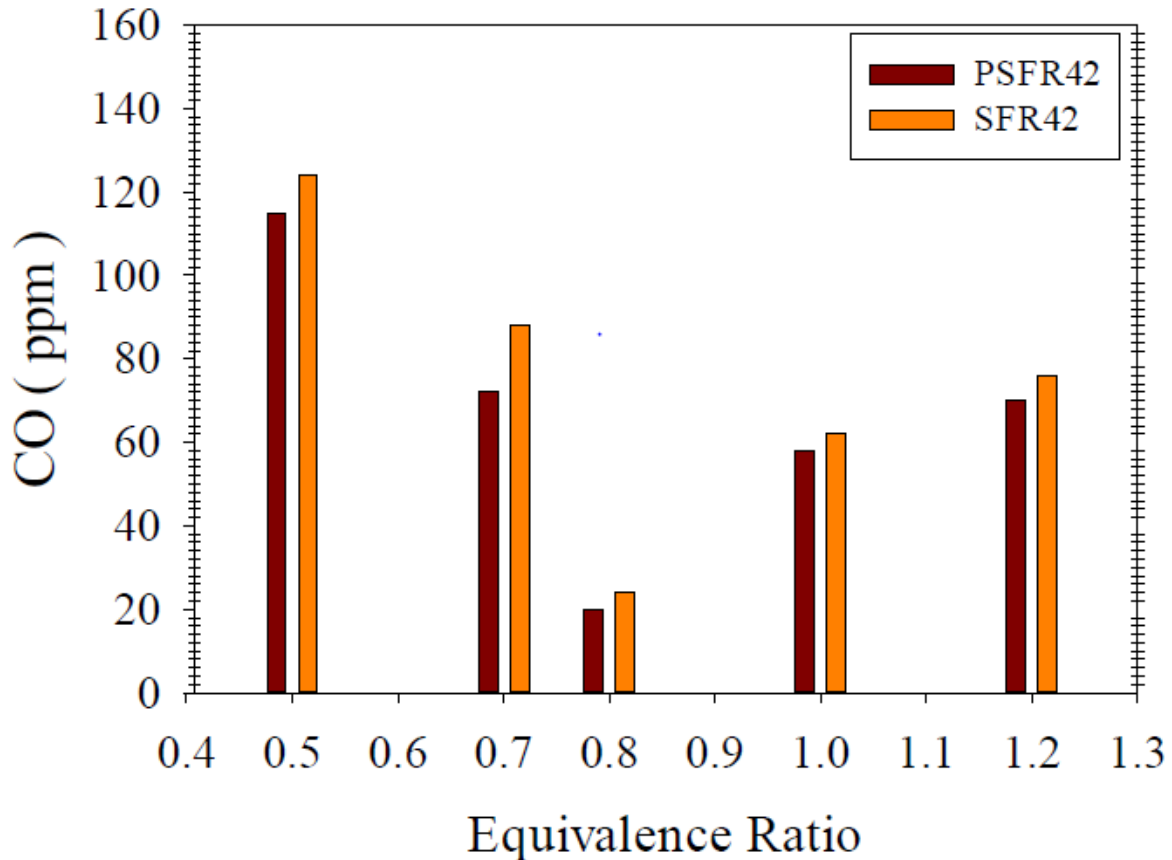


FIGURE 10. Average CO concentrations plotted against equivalence ratio for cases with and without preheated tangential air, PSFR42 and SFR42.

CONCLUSION

This work used an asymmetric swirling flameless combustor with natural gas as the fuel in order to understand the effect of preheating and also to observe the effect of swirling in a combustor system experimentally. It was observed that combustor design plays a vital role in achieving flameless combustion without using a diluent such as CO₂, H₂O, N₂, or Ar. Six different cases i.e. SFR2, SFR4, SFR42, PSFR2, PSFR4 and PSFR42 were investigated, where SFR42 stands for a swirling flameless combustor with four tangential air inlets, 12 axial air inlets, and 11 coaxial fuel inlets and SFR42 was found to be the best configuration for the combustor in order to achieve flameless combustion and low emissions. In the case of SFR42, NO_x and CO emissions are lowest at lean conditions with an equivalence ratio of 0.8, equaling 3 ppm and 24 ppm, respectively. Thermal efficiency was found to have increased by about 10% for PSFR42 when compared to the non-preheated SFR42. Temperature homogeneity was investigated for all the six (6) cases in swirling flameless combustion and was found to be 0.03, 0.04, and 0.03, respectively. These findings suggest that the temperature within the combustion chamber is relatively the same, which is a key feature of flameless combustion. This research also showed that swirling flameless combustion may be achieved with or without preheated tangential air. Preheated air has aided in the improvement of thermal efficiency in general. However, this comes at the cost of an increase in NO_x emissions.

REFERENCES

1. A.A.A. Abuelnuor, M.A. Wahid, S.E. Hosseini, A. Saat, K.M. Saqr, H.H. Sait, M. Osman, Characteristics of biomass in flameless combustion: A review, *Renew. Sustain. Energy Rev.* 33 (2014) 363–370. <https://doi.org/10.1016/j.rser.2014.01.079>.
2. N. M. M., W. Andrew P., Y. T. F., MILD Combustion: A Technical Review Towards Open Furnace Combustion, *Int. J. Automot. Mech. Eng.* 6 (2012) 731–752.
3. S. Achinas, V. Achinas, G.J.W. Euverink, A Technological Overview of Biogas Production from Biowaste, *Engineering*. 3 (2017) 299–307. <https://doi.org/10.1016/J.ENG.2017.03.002>.
4. R.A. Alwan, *Thermal and Fluid Flow Analysis of Swirling Flameless Combustion*, Universiti Teknologi Malaysia, 2016.
5. S.E. Hosseini, M.A. Wahid, S. Salehirad, Environmental protection and fuel consumption reduction by flameless combustion technology: A review, *Appl. Mech. Mater.* 388 (2013) 292–297. <https://doi.org/10.4028/www.scientific.net/AMM.388.292>.
6. R. Raj, A. Chaurasia, Flameless Combustion: A Review, *IJSTE-International J. Sci. Technol. Eng.* |. 3 (2016) 70–75. www.ijste.org.
7. S.E. Hosseini, M.A. Wahid, A.A.A. Abuelnuor, Biogas flameless combustion: A review, *Appl. Mech. Mater.* 388 (2013) 273–279. <https://doi.org/10.4028/www.scientific.net/AMM.388.273>.
8. K. Adam, M.A. Wahid, On the effects of tangential air inlets distribution configurations to the combustion characteristics of a direct injection liquid fueled swirl flameless combustor (Sfc), *Evergreen*. 8 (2021). <https://doi.org/10.5109/4372267>.
9. N. Romero-Anton, X. Huang, H. Bao, K. Martin-Eskudero, E. Salazar-Herran, D. Roekaerts, New extended eddy dissipation concept model for flameless combustion in furnaces, *Combust. Flame*. 220 (2020) 49–62. <https://doi.org/10.1016/j.combustflame.2020.06.025>.
10. R.A. Alwan, M.A. Wahid, M.F.M. Yasin, A.K.A.Y. Al-Taie, A.A.A. Abuelnuor, Effects of equivalence ratio on asymmetric vortex combustion in a Low NO_x Burner, *Int. Rev. Mech. Eng.* 9 (2015) 476–483. <https://doi.org/10.15866/ireme.v9i5.7157>.
11. N. Kim, Y. Kim, M.N.M. Jaafar, M.R. Rahim, M. Said, Effects of hydrogen addition on structure and NO formation of highly CO-Rich syngas counterflow nonpremixed flames under MILD combustion regime, *Int. J. Hydrogen Energy*. 46 (2021) 10518–10534. <https://doi.org/10.1016/j.ijhydene.2020.12.120>.
12. F. Xing, A. Kumar, Y. Huang, S. Chan, C. Ruan, S. Gu, X. Fan, Flameless combustion with liquid fuel: A review focusing on fundamentals and gas turbine application, *Appl. Energy*. 193 (2017) 28–51. <https://doi.org/10.1016/j.apenergy.2017.02.010>.
13. R. Weber, A.K. Gupta, S. Mochida, High temperature air combustion (HiTAC): How it all started for applications in industrial furnaces and future prospects, *Appl. Energy*. 278 (2020) 115551. <https://doi.org/10.1016/j.apenergy.2020.115551>.
14. W.A.P. and Y.T. Noor M. M., Effect of Air-Fuel Ratio on Temperature Distribution and Pollutants for Biogas Mild Combustion, 10 (2014) 1980–1992.
15. B.B. Dally, E. Riesmeier, N. Peters, Effect of fuel mixture on moderate and intense low oxygen dilution combustion, *Combust. Flame*. 137 (2004) 418–431. <https://doi.org/10.1016/j.combustflame.2004.02.011>.
16. A.A.A. Abuelnuor, M.A. Wahid, A. Saat, M.M. Sies, M.K. Elbasheer, S.E. Hosseini, A.G. Dairobi, H.A. Mohammed, A.N. Darus, Review of numerical studies on NO_x emission in the flameless combustion, *Appl. Mech. Mater.* 388 (2013) 235–240. <https://doi.org/10.4028/www.scientific.net/AMM.388.235>.

17. J.A. Wüning, J.G. Wüning, Flameless oxidation to reduce thermal no-formation, *Prog. Energy Combust. Sci.* 23 (1997) 81–94. [https://doi.org/10.1016/s0360-1285\(97\)00006-3](https://doi.org/10.1016/s0360-1285(97)00006-3).
18. A. Cavigiolo, M.A. Galbiati, A. Effuggi, D. Gelosa, R. Rota, Mild combustion in a laboratory-scale apparatus, *Combust. Sci. Technol.* 175 (2003) 1347–1367. <https://doi.org/10.1080/00102200302356>.
19. H.S. Gitar, Y.A. Eldrainy, Design and investigation of a central air jet flameless combustor, *Alexandria Eng. J.* 60 (2021) 2291–2301. <https://doi.org/10.1016/j.aej.2020.12.035>.
20. A.E.E. Khalil, A.K. Gupta, Swirling distributed combustion for clean energy conversion in gas turbine applications, *Appl. Energy.* 88 (2011) 3685–3693. <https://doi.org/10.1016/j.apenergy.2011.03.048>.
21. V. Mahendra Reddy, S. Kumar, Development of high intensity low emission combustor for achieving flameless combustion of liquid fuels, *Propuls. Power Res.* 2 (2013) 139–147. <https://doi.org/10.1016/j.jprr.2013.04.006>.
22. K.M.M.E.M. Saqr., Aerodynamics and Thermochemistry of Turbulent confined Asymmetric Vortex Flames. A thesis submitted in fulfillment of the requirements for the award of the degree of Doctor of Philosophy (Mechanical Engineering), (2011) 1–226.